JACS
JOURNAL OF THE AMERICAN CHEMICAL SOCIETY

Article

pubs.acs.org/JACS

Propensity of Hydrated Excess Protons and Hydroxide Anions for the Air−Water Interface

Ying-Lung Steve Tse,[†] Chen Chen,[†,‡] Gerrick E. Lindberg,[§] Revati Kumar,[∥] and Gregory A. Voth*[,†]

[†]Department of Chemistry, James Franck Institute, Institute for Biophysical Dynamics, and Computation Institute, The University of Chicago, Chicago, Illinois 60637, United States

[‡]College of Chemistry and Molecular Sciences, Hubei Key Lab of Electrochemical Power Sources, Wuhan University, Wuhan 430072, China

[§]Department of Chemistry and Biochemistry, Northern Arizona University, Flagstaff, Arizona 86011, United States

[∥]Department of Chemistry, Louisiana State University, Baton Rouge, Louisiana 70803, United States

Supporting Information

ABSTRACT: Significant effort has been undertaken to better understand the molecular details governing the propensity of ions for the air−water interface. Facilitated by computationally efficient reactive molecular dynamics simulations, new and statistically conclusive molecular-scale results on the affinity of the hydrated excess proton and hydroxide anion for the air−water interface are presented. These simulations capture the dynamic bond breaking and formation processes (charge defect delocalization) that are important for correctly describing the solvation and transport of these complex species. The excess proton is found to be attracted to the interface, which is correlated with a favorable enthalpic contribution and consistent with reducing the disruption in the hydrogen bond network caused by the ion complex. However, a recent refinement of the underlying reactive potential energy function for the hydrated excess proton shows the interfacial attraction to be weaker, albeit nonzero, a result that is consistent with the experimental surface tension measurements. The influence of a weak hydrogen bond donated from water to the protonated oxygen, recently found to play an important role in excess hydrated proton transport in bulk water, is seen to also be important for this study. In contrast, the hydroxide ion is found to be repelled from the air−water interface. This repulsion is characterized by a reduction of the energetically favorable ion−water interactions, which creates an enthalpic penalty as the ion approaches the interface. Finally, we find that the fluctuation in the coordination number around water sheds new light on the observed entropic trends for both ions.

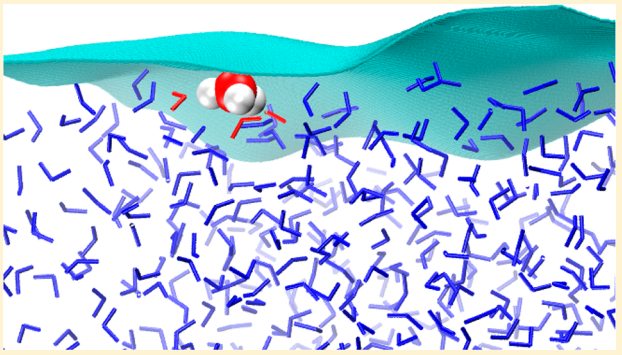

INTRODUCTION

The air−water interface has received considerable attention not just because of its importance for many atmospheric and environmental processes, but also as a simplified model of the hydrophobic−hydrophilic interfaces.[1,2] Despite this attention, the behavior of ions near the air−water interface remains ambiguous, and several aspects of their behavior are unresolved. In particular, the acidic or basic nature of the air−water interface as a function of bulk solution pH has been a frequent topic of research, with relevance for understanding numerous important processes.[1,2]

It was first predicted by our group 11 years ago that hydrated excess protons are attracted to the air−water interface, at least under mildly acidic conditions.[3] This behavior contrasts the classical view from continuum electrostatics of Samaras and Onsager.[4] Surface selective spectroscopies have generally supported the presence of excess protons at the interface, although the evidence can be indirect.[5−8] Changes in spectra collected in sum-frequency generation (SFG) experiments have been attributed to a perturbation of the surface hydrogen bond network by the hydrated excess proton, although there has also been debate about the precise interpretation. Subsequent comparisons of molecular dynamics (MD) simulations and SFG experiments have supported the view that excess protons accumulate at the air−water interface.[9,10] The change in surface tension of salt versus weak acid solutions at the air−water interface analyzed with a surface-bulk partitioning model have likewise suggested a weak attraction of protons to the interface.[11] The original reactive molecular dynamics simulations and subsequent ones from our group,[3,12,13] all using the multistate empirical valence bond (MS-EVB)[14−16] reactive MD method, have suggested a molecular rationale for the excess proton affinity for the air−water interface.[3,13] This conclusion is based on the disruption of the hydrogen-bond network in water by the hydrated excess proton, resulting in the Eigen cation

Received: July 11, 2015
Published: September 14, 2015

DOI: 10.1021/jacs.5b07232
J. Am. Chem. Soc. 2015, 137, 12610−12616

structure ($H_9O_4^+$) being somewhat more stable at the interface than the bulk.[13] Additional simulation on water clusters with cations[17] suggested dramatically different behavior for hydrated protons than for Na^+ ions above the cluster melting point, with the latter being on the surface of the cluster and the former in the interior.

While these studies have corroborated that the excess proton has some propensity for the air−water interface, the magnitude of that attraction has varied, and there remains considerable debate about the binding strength $\Delta F_{binding}$ of the excess proton to the air−water interface. Studies can be generally divided into those that predict a weak attraction to the air−water interface ($\Delta F_{binding} < k_BT$),[2,5,18,19] and those that predict a stronger attraction ($\Delta F_{binding} > k_BT$).[3,12,13,20−25] One explanation of this discrepancy appears to be an underestimation of the importance of the hydronium form of the hydrated excess proton as a hydrogen-bond acceptor.[2,26] Berkelbach, Lee, and Tuckerman studied the solvation and transport mechanism of the excess proton in water with BLYP-based ab initio molecular dynamics (AIMD) simulations.[27] They stressed the importance of a weak hydrogen bond donated from a water hydrogen (H_w) to the oxygen most closely associated with the excess proton hydronium-like structure (O*).[27,28] Jagoda-Cwiklik and co-workers compared the affinity of excess proton for the air−water interface using a polarizable force field with and without an interaction dedicated to this H_w−O* hydrogen bond.[26] The H_w−O* interaction is represented by a Lennard-Jones potential fit to a CCSD(T) potential energy scan of this hydrogen bond.[26] The CCSD(T) scan in the gas-phase cluster yields a different minimum location than is seen in the condensed phase AIMD simulations, and the corresponding peak in the H_w−O* radial distribution function (RDF) from the resulting force field is displaced relative to the AIMD.[26,28] Nevertheless, they found that the O*−H_w interaction dramatically reduces the affinity of the proton for the air−water interface from −1.8 ± 0.5 kcal/mol (or −3 ± 1 kcal/mol from a study by Vacha et al.[20]) to −0.2 ± 0.5 kcal/mol.[26] Baer and co-workers[2] performed BLYP based AIMD simulations of the H^+ at the air−water interface and observed this transient O*−H_w hydrogen bond, and that the excess proton is equally likely at the interface as in the bulk, although there is large statistical error in such simulations, as well as uncertainties from the inaccuracies in the underlying density functional theory for water.

Similar to the excess proton, it has also been challenging to determine the propensity of the hydroxide anion for the air−water interface. Most notably the motion of bubbles and droplets in oil and water in electrophoresis studies has shown a negative surface charge that is attributed to the presence of the hydroxide ions.[29−31] However, it is not clear how deep the "surface" is in these experiments, and moreover, surface tension measurements have revealed the hydroxide ion is excluded from the air−water interface.[19] The macroscopic scale of these experiments makes it difficult to unambiguously identify the molecular origins of this behavior. AIMD simulations have supported the accumulation of the hydroxide ion at the air−water interface,[2,32] though other calculations have predicted the repulsion of the anion.[21,25,33] Simulations by Wick and Dang[34,35] suggested that the hydroxide ion has no preference for the interface, but was repelled when a sodium counterion is present.[35] Some polarizable classical MD simulations predicted the attraction of this ion to the interface, though similar simulations found the ion is repelled from the interface.[9,21,33] Surface selective spectroscopies have predicted repulsion of the hydroxide ion from the air−water interface,[9,36,37] and classical MD simulations used to compute SFG spectra were able to reproduce experimental spectra, thus, strengthening the argument that the hydroxide ion is repelled from the surface.[38] The general discrepancies between these studies remain unresolved,[39,40] and the contradictory hydroxide results from nonreactive classical MD simulations that do not include the Grotthuss proton shuttling mechanism cannot in principle describe the correct solvation and dynamics of these hydrogen-bonded networks, and can unfortunately lead to confusion in this challenging problem.

Clearly, computer simulations can play an important role in elucidating molecular details of the affinity of ions for the air−water interface. Simulations using conventional force fields are an attractive option because of their modest computational cost, but they are commonly restricted to the fixed bonding topology defined at the beginning of the simulations. This means that the breaking and forming of chemical bonds necessary for structural transport of protonic defects (Grotthuss mechanism[41]) is not feasible. AIMD simulations are a natural choice for chemically reactive systems because electronic degrees of freedom are explicitly treated. While they have provided valuable information about the air−water interface, their significant computational expense limits the accessible simulation time and size. In addition to limitations arising from small system sizes and short simulation times, the majority of AIMD simulations for this type of system estimate exchange-correlation with the generalized gradient approximation, often employing the BLYP functional, which has been shown to predict a water melting point well above room temperature.[42,43] Consequently, BLYP-based AIMD is expected to result in glassy and overstructured water dynamics at 300 K,[28] which will complicate the comparison of AIMD with experiment.

To circumvent these challenges, methods that bridge the efficiency of conventional MD with the accuracy of quantum-based methods have been developed. In this work, this is achieved with multiscale reactive molecular dynamics (MS-RMD) simulations[44] of the hydroxide ion and the hydrated excess proton. MS-RMD provides an atomistic perspective of ion dynamics, while being capable of describing both standard vehicular and structural transport of protonic defects.

■ SIMULATION DETAILS

In the MS-RMD and earlier MS-EVB methods, which are described in detail elsewhere,[14,44] the state of the system is represented by a linear combination of the basis states $|i\rangle$, each of which maps onto a single covalent bonding topology and is coupled to other states via off-diagonal Hamiltonian matrix elements, which facilitate proton transfer reactions. At each time step, the components c_i of the ground state eigenvector of the Hamiltonian matrix are used to compute atomistic forces by the Hellman-Feynman theorem. This protonic charge defect is delocalized over multiple molecules, the location of which changes continuously throughout the simulation in response to environmental influences. Delocalization of the charge defect over the states in the hydrated complex changes the average atomic partial charges, resulting in an effective polarization.

For analyzing an MS-RMD simulation, it is useful to define a continuous collective coordinate that represents the time-dependent location of the protonic defect. The center of excess charge (CEC) is an average of the atomic coordinates of the reactant molecule in each basis state, weighted by the probability of that state. The CEC is defined as

DOI: 10.1021/jacs.5b07232
J. Am. Chem. Soc. 2015, 137, 12610−12616

$$r_{CEC} = \sum_{i=1}^{N} c_i^2 r_{i,COC} \quad (1)$$

where c_i and $r_{i,COC}$ are the probability amplitude and the position vector of the center of charge for the ith state. Therefore, the CEC is a weighted average of the positions of the centers of charge over the basis states.

The excess proton interaction potential is described using the newly developed MS-EVB 3.2 hydrated excess proton model. As was discussed in the Introduction, AIMD simulations have revealed the importance of H_3O^+ serving as a weak hydrogen-bond acceptor. The MS-EVB 3.2 proton model was therefore developed to include the effect of this weak O*− H_w hydrogen bond. The functional form of the 3.2 model is the same as that of the 3.0 model,[16] except for the addition of a Lennard-Jones interaction between O* and H_w. The 3.2 model was parametrized using the same MP2 gas-phase cluster energies as was used to develop the 3.0 model,[16] the MP2 potential energy scans for the Eigen ion, as well as the O*−H_w radial distribution function obtained from condensed phase AIMD simulations. These AIMD simulations were carried out using the BLYP functional along with the Grimme dispersion correction[45] and the TZV2P basis set. These BLYP data were used to parametrize only the interactions between the hydronium and the fourth water. One might question our choice of using BLYP data, seemingly incompatible with our criticism of the properties of BLYP bulk water. However, any problems with the BLYP water-hydronium statistical properties such as the RDFs are much less severe and compare reasonably well with the available experimental data.[28,46] The parameters of the MS-EVB 3.2 model, some of which are different from those of the 3.0 model, are provided in the Supporting Information. Unless otherwise specified, the proton model discussed in the paper is the MS-EVB 3.2 model.

The hydroxide model studied in this paper is based on the original MS-RMD paper.[44] The two most important differences between the new hydroxide model and the original model are (1) the use of Lennard-Jones 12-6 potentials for pairwise interactions in the new model instead of tabulated potentials to ensure greater transferability, and (2) the use of an anharmonic water model aSPC/Fw,[47] instead of SPC/Fw,[48] for more accurate water O−H bond energy calculations during proton transfer in which the water bonds are stretched and can lead to unphysically large forces if purely harmonic bonds are used. Unlike the case of the hydrated proton, the stretching energy of water O−H bonds is very important for the hydroxide model. The new parameters and other details of the hydroxide model are provided in the Supporting Information.

All of the simulations described here contain a slab of 999 water molecules with either a hydronium or a hydroxide ion. These simulations with only one ion aim to understand the intrinsic preference of the individual ion for the interface at low concentrations. Without a thorough understanding of this simple but by no means straightforward scenario, any additional effects that may arise from the presence of other ions (like ions and counterions) at higher concentrations cannot be readily understood. The water model used for the proton models is SPC/Fw and that for the hydroxide model is aSPC/Fw. The thickness of the water slab is about 30 Å. The simulation cell is fully periodic with dimensions 31.07 × 31.07 × 100 $Å^3$. Simulations were performed using a modified version of the LAMMPS MD code.[49] Long-ranged electrostatic interactions were calculated using the Particle−Particle-Particle-Mesh (P^3M) method[50] with a relative error in forces of 10^{-5}. A time step of 0.5 fs was used and the *NVT* (constant number of particles, volume, and temperature) ensemble was maintained with a Nosé−Hoover thermostat with a relaxation constant of 100 fs.

The direction of the normal of the air−water interface is defined to be the z-direction, and z = 0 is assigned to the position of the Gibbs dividing surface (GDS), which is an idealized, zero-volume plane separating the two phases. The z variable in a function presented in this paper always means the average z coordinate of the CEC from the GDS. The potentials of mean force (PMF) were calculated with the umbrella sampling method and the weighted histogram analysis method (WHAM).[51,52] The CEC coordinate was restrained at distances of 5−18 Å from the system center of mass in the z-direction in a total of 14 evenly spaced windows. The harmonic force constant of the restraining potential was 5.0 kcal mol^{-1} $Å^{-2}$. In each of the 14 windows, 20 independent 1 ns trajectories of production data were collected.

RESULTS AND DISCUSSION

1. Surface Propensity. To study surface propensity of the ions, we calculate the potential of mean force ΔF as a function of the average CEC z coordinate, and the results are shown in Figure 1. These results reveal that the hydrated proton is weakly attracted to the interface, while the hydroxide ion is repelled. The hydroxide ion is repelled from the GDS (z = 0 Å) by about 2.4 kcal/mol, whereas the excess proton PMF shows a well depth of −0.55 kcal/mol. Compared to previous study of the proton 3.0 model, the 3.2 model has a smaller well depth (−0.55 vs −1.8 kcal/mol) due to the presence of an explicit O*−H_w pairwise interaction in the 3.2 model. These results are qualitatively consistent with the recent work by Duignan, Parsons, and Ninham using continuum modeling,[25] even though they predict a stronger surface attraction, like our previous 3.0 model, for the hydrated excess proton. One important difference between their continuum model and our present proton model is that the former, like our previous 3.0 model, does not explicitly incorporate the effect of the fourth water neighbor that is a weak hydrogen-bond donor to the hydronium. We should also note that our findings for the ion propensities for the surface may appear to be similar as those by van der Spoel and co-workers[33] using nonreactive classical polarizable models. However, upon closer inspection, the features of the simulations as well as our results are clearly different, in addition to their omission of the essential Grotthuss proton hopping and charge defect delocalization physics. Certain comparisons between our results and theirs are provided in the Supporting Information.

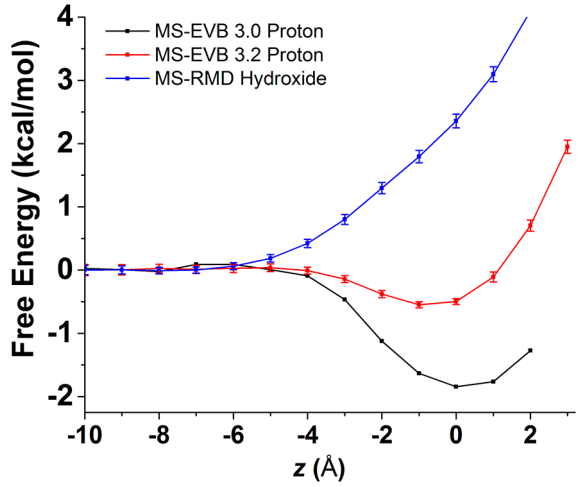

Figure 1. PMFs for the MS-EVB 3.0 hydrated excess proton model (black), the MS-EVB 3.2 model (red), and the MS-RMD hydroxide model (blue) as a function of the CEC average z displacement from the GDS. The data points for the 3.0 model were extracted from ref 13. The error bars were obtained using bootstrapping in WHAM by assuming the correlation time is 10 ps.

DOI: 10.1021/jacs.5b07232
J. Am. Chem. Soc. 2015, 137, 12610−12616

To better understand the observed trends in the free energy, it is decomposed into enthalpic and entropic contributions as described next.

2. Free Energy Decomposition. The free energy is first decomposed into entropic, $-T\Delta S$, and enthalpic, ΔH, contributions using a finite difference between PMFs calculated at 280 and 320 K. In the calculation, we assume both changes of the entropy and the enthalpy are temperature-independent in this temperature range, so that there is a linear relationship in the temperature T among the changes in free energy, entropy, and enthalpy: $\Delta F(z,T) = \Delta H(z) - T\Delta S(z)$ for every z.

On the other hand, a local decomposition scheme, similar to that of Otten et al.[53] for simple monatomic ions, was developed for the hydrated excess proton in our previous study.[13] It is further modified here to study the different contributions to the enthalpic term for both the hydrated excess proton and the hydroxide ion. The local energy is written as

$$\Delta H_{\text{local}}(z) = \Delta U_{\text{ww}}(z) + \Delta U_{\text{iw}}(z) + \Delta U_{\text{OD}}(z) \tag{2}$$

where Δ is the difference from the value at $z = -10$ Å, $U_{\text{OD}}(z)$ is the average off-diagonal contribution in the multistate formalism, $U_{\text{ww}}(z)$ and $U_{\text{iw}}(z)$ are the water−water (ww) and ion−water (iw) interaction energies in the system, respectively. The $U_{\text{ww}}(z)$ and $U_{\text{iw}}(z)$ are sums of the water−water E_{ww} and ion−water E_{iw} energies *per molecule* in three different regions [coordination shell (c), interface (i), and bulk (b)]:

$$U_{\text{ww}}(z) = \frac{1}{2}\sum_{x\in\{\text{c,i,b}\}} \langle n(z)\rangle_x \langle E_{\text{ww}}(z)\rangle_{x,\text{states}} \tag{3}$$

$$U_{\text{iw}}(z) = \sum_{x\in\{\text{c,i,b}\}} \langle n(z)\rangle_x \langle E_{\text{iw}}(z)\rangle_{x,\text{states}} \tag{4}$$

where n is the number of water molecules, $\langle ...\rangle_x$ is an ensemble average in the x region (c, i, or b), and $\langle ...\rangle_{x,\text{states}}$ is an ensemble average in the x region over the basis states. Note the energies per molecule (E_{ww} and E_{iw}) are made more general than the original formulation and can now depend on z. Including the z-dependence is found to improve the agreement between the local decomposition and finite difference methods.[54] The reader is referred to the Supporting Information for the definitions of the three regions and more details of how these energy terms are defined and calculated. Once the enthalpic contribution is determined, the entropic contribution $-T\Delta S_{\text{local}}$ is then determined by $\Delta F - \Delta H_{\text{local}}$.

The decomposition of the free energy into entropic and enthalpic contributions is shown in Figure 2. It is reassuring that the finite-difference (subscript "finite-diff") and the local decomposition (subscript "local") methods agree qualitatively. Note that in the discussion that follows, the sign of the entropic contribution can be confusing because of the $-T$ factor. From here onward in this paper, entropic contribution is always $-T\Delta S$, whereas entropy change is ΔS, with the opposite sign.

It is clear in Figure 2 that the repulsion of the hydroxide ion from the interface is the result of an enthalpic penalty (blue in Figure 2) because the entropic contribution $-T\Delta S$ (red) is negative and favorable (positive ΔS). On the other hand, the enthalpic contribution favors the presence of the hydrated excess proton at the interface even though its entropic contribution is positive and unfavorable (negative ΔS). Although the local energy decomposition is more approximate than the finite difference method, the former can provide

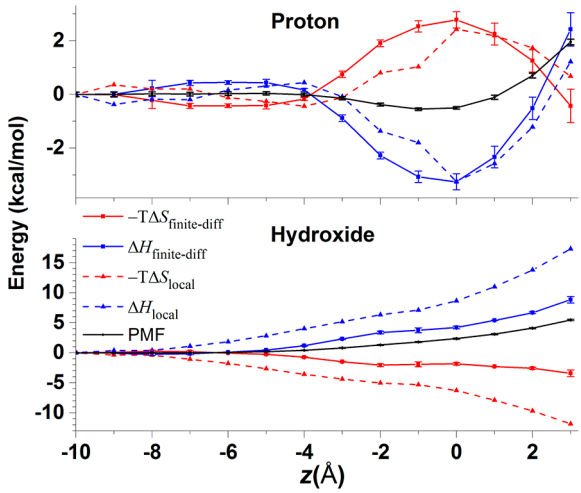

Figure 2. PMFs for the excess proton and the hydroxide and their decompositions into the enthalpic (blue) and entropic (red) contributions using both the finite difference method (solid line) and the local energy decomposition method (dash line) as a function of the CEC average z displacement from the GDS.

insightful molecular details for explaining the surface propensity as we shall see next.

2.1. Enthalpic Contributions. We found that $U_{\text{OD}}(z)$ in eq 2 does not depend strongly on z; so, to a good approximation, the local enthalpy change ΔH_{local} is the sum of both changes in the *total* water−water ΔU_{ww} and the *total* ion−water ΔU_{iw} interaction energies:

$$\Delta H_{\text{local}}(z) \approx \Delta U_{\text{ww}}(z) + \Delta U_{\text{iw}}(z) \tag{5}$$

where these changes in energy are relative to their values at $z = -10$ Å, far from the interface.

These energy changes are plotted in Figure 3. For a hydrated excess proton, we see that ΔU_{ww} follows ΔH_{local} closely, and it, therefore, shows that the trend of ΔH_{local} in Figure 2 is caused by the change in the water−water interactions. Through a closer inspection on the individual energy terms (see

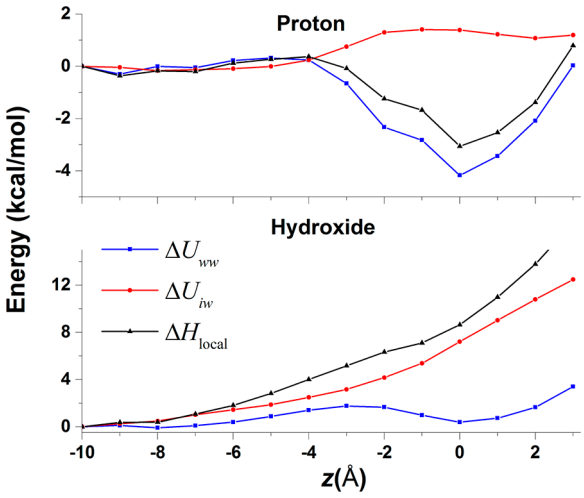

Figure 3. Energy change, relative to their $z = -10$ Å value, for the total water−water (ΔU_{ww}) and the total ion−water (ΔU_{iw}) interaction energies as a function of the CEC average z displacement from the GDS. To a good approximation, the enthalpic contribution (ΔH_{local}) is the sum of the two kinds of interactions.

DOI: 10.1021/jacs.5b07232
J. Am. Chem. Soc. 2015, 137, 12610−12616

Supporting Information), we found that the observed energy minimum is caused by an increased number of water in the bulk region $\langle n\rangle_b$, which causes a more negative water−water interaction energy in the region $\langle n\rangle_b\langle E_{ww}\rangle_{b,states}$, as the disruption in the hydrogen bond network caused by the presence of the excess proton in the region diminishes. It is interesting to note that, as the excess proton approaches the surface, even though the ion−water interaction energy in the interfacial region $\langle n\rangle_i\langle E_{iw}\rangle_{i,states}$ becomes more negative, it is almost completely balanced by the more positive ion−water interaction energy in the bulk $\langle n\rangle_b\langle E_{iw}\rangle_{b,states}$.

For the hydroxide, ΔU_{iw} is largely responsible for the trend in ΔH_{local}. The individual energy contributions (see Supporting Information) show that the increase in ΔH_{local}, as the ion approaches the interface, is mainly caused by the more positive ion−water interaction energy in the bulk. Even though the water−water interaction energy in the bulk region becomes more negative, it is not enough to overcome the increasingly positive ion−water interaction energy.

2.2. Entropic Contribution. Because there does not exist a straightforward analogous local decomposition scheme for the entropy change, it is more challenging to understand the origin of an entropic contribution on a molecular level. We approach this problem by studying two different kinds of fluctuations in the systems that can shed light on the observed trends for the entropic contributions.

2.2.1. Fluctuation in Surface Height. While the GDS is useful to provide an average description of the boundary between phases, it is not sufficient to reveal local, molecular-scale perturbations. Therefore, the interface is examined with the instantaneous interface method as defined by Willard and Chandler.[55,56]

The fluctuation of the interface can be described by a similar scheme used in our previous study[13] that is based on the work of Otten et al.[53] For a given z window of the CEC, the fluctuation of the interface is defined to be the variance in height $\delta h(r_p)^2$:

$$\delta h(r_p)^2 = \langle [h(r_p) - \langle h(r_p)\rangle]^2\rangle \quad (6)$$

where $h(r_p)$ is the vertical height of the instantaneous interface at a perpendicular distance r_p in the xy-plane from the CEC. To make it easier to compare the fluctuations within the same system, the variance is normalized by $\delta h(r_0)^2$ with r_0 = 21.75 Å.

The normalized fluctuation in the instantaneous surface height $\delta h(r_p)^2/\delta h(r_0)^2$ as a function of r_p and z is plotted in Figure 4. As shown by the blue/green domain for small r_p values, both the excess proton and the hydroxide are found to pin the interface, reducing $\delta h(r_p)^2/\delta h(r_0)^2$ to less than 1. It is clear that the pinning effect is stronger and more long-ranged for the excess proton than the hydroxide. However, in both cases, $\delta h(r_p)^2/\delta h(r_0)^2 < 1$ for small r_p indicates a positive entropic contribution ($-T\Delta S$), but this unfortunately is not consistent with the observed negative entropic contribution for the hydroxide case.

2.2.2. Fluctuation in Coordination Number of Water. The enthalpic contribution from the local energy decomposition hints at the importance of the water−water interactions. This leads us to investigate the fluctuation (variance) of the number of water neighbors in the first solvation shell (3.2 Å radius) of a water molecule $\delta N_w(z)^2$. The normalized fluctuation $\delta N_w(z)^2/\delta N_w(z_0)^2$ (with z_0 = −10 Å) is plotted in Figure 5. The initial rise of both curves up to z = −4 Å, indicating a negative

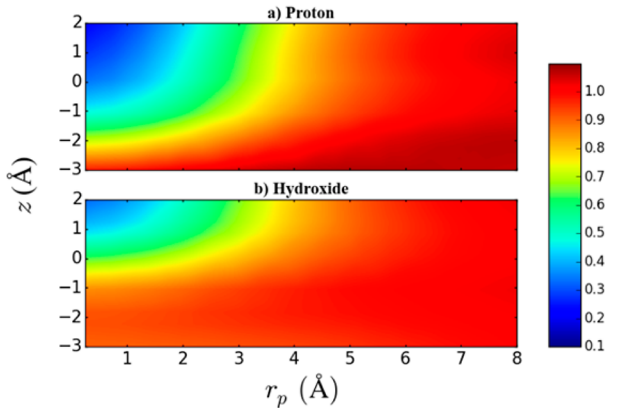

Figure 4. Normalized fluctuation of the instantaneous surface height $\delta h(r_p)^2/\delta h(r_0)^2$ as a function of perpendicular distance r_p from the CEC and the CEC average z displacement from the GDS. r_0 is chosen to be 21.5 Å. When the normalized value is smaller than 1, it means the region is pinned by the ion, resulting in a positive entropic contribution ($-T\Delta S$).

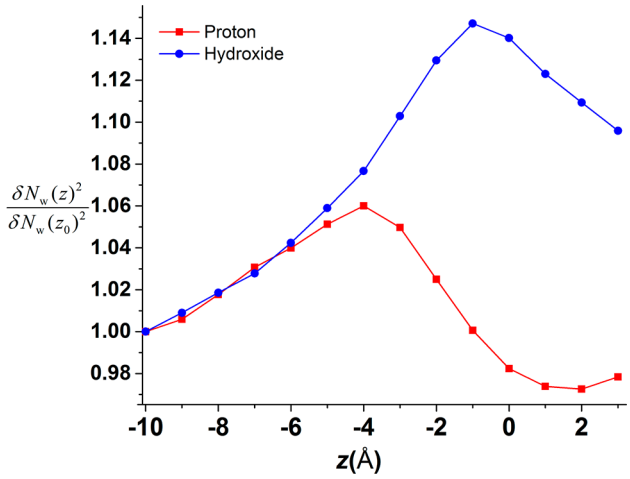

Figure 5. Normalized fluctuation of the coordination number of water in the first solvation shell $\delta N_w(z)^2/\delta N_w(z_0)^2$ as a function of the average z displacement of the CEC (not of the water) from the GDS. z_0 is chosen to be −10 Å. A value greater than 1 means the entropic contribution ($-T\Delta S$) is negative (positive ΔS).

entropic contribution ($-T\Delta S$), is consistent with $-T\Delta S_{finite\text{-}diff}$ in Figure 2 for both the excess proton and the hydroxide. Following the proton curve to greater z values in Figure 5, we find that the eventual fall to a value below 1 is consistent with the positive sign of the entropic contribution (or negative ΔS) up to about z = 0 Å in Figure 2. On the other hand, the normalized fluctuation in N_w for the hydroxide curve in Figure 5 continues to stay above 1, indicating a persistent positive entropic contribution. The slope of the hydroxide curve eventually becomes negative, and this roughly corresponds to the flatter slope of the $-T\Delta S$ hydroxide curve starting at about z = −2 Å in Figure 2. These results suggest an important connection between the fluctuation in the coordination number and the entropic contribution from z = −10 Å to about 0 Å. Both the entropic contributions for the proton and hydroxide in Figure 2 become more negative beyond z = 0 Å, indicating an increasing trend for ΔS. This observation is consistent with the increasing configurational entropy for the ion complex as it enjoys more freedom in the air region.

DOI: 10.1021/jacs.5b07232
J. Am. Chem. Soc. 2015, 137, 12610−12616

CONCLUSIONS

This work has examined the molecular features that give rise to the behavior of the hydrated excess proton and the hydroxide ion at the air−water interface with the newly developed proton and the hydroxide reactive MD models. These models allow us to perform analyses that require trajectories so long that it would be difficult for AIMD methods to collect statistically converged results for these chemically reactive systems, let alone to describe the systems accurately.

The hydroxide ion is found to be enthalpically repelled from the interface, which is correlated with a reduction in the energetically favorable ion−water interactions. This result is consistent with the resonant UV second harmonic generation experimental data by Petersen and Saykally that are best reproduced by a Langmuir adsorption model with hydroxide being repelled from the surface.[37]

It has also been previously reported by Tobias and Mundy[2,32] that the water coordination number around a hydroxide ion is an important factor and can influence the ion propensity for the interface. However, even though the coordination number of our hydroxide model changes from about 4.2 to 3.3 in going from bulk to the interface, consistent with the coordination number trend reported by Tobias and Mundy, our present result is that hydroxide is repelled from the surface, whereas they found the hydroxide is slightly attracted to the surface. These different results indicate that the change in the coordination number alone is not the determining factor. Instead, we believe the fluctuations in the coordination number of water, first reported in this work, are much more strongly correlated to the observed trends. The coordination numbers for both the hydroxide and the hydronium are provided in the Supporting Information.

The excess proton, on the other hand, is found to be weakly attracted to the interface due to a favorable enthalpic contribution that is correlated with eliminating the disruption in the hydrogen bond network caused by the ion complex in the bulk region. The absence of the hydrated excess proton in the bulk region leads to an increased number of water−water interactions that gives rise to a negative and energetically favorable enthalpic contribution.

The different fluctuations in the system provide some clues to the origin of the observed entropic contributions. However, the fluctuation in the instantaneous surface height predict incorrectly that the entropic contribution ($-T\Delta S$) for the hydroxide would be positive, whereas we find that there is a clearer connection between the fluctuation in the coordination number of water and the observed entropic trends for both ions.

The work of Pegram and Record[18,19] provides experimental evidence that hydrated excess protons are weakly surface-accumulated. They estimate that the ratio of the surface proton concentration to that of the bulk is about 1.5, which leads to a free energy difference of about 0.4 k_BT. This result is semiquantitatively consistent with our predicted free energy difference of about 1 k_BT by the new hydrated proton model. This also shows the importance of the added relatively weak O*−H_w hydrogen-bond, which is correlated with the reduction of the free energy well depth from 3 k_BT in the earlier model.[13,16]

ASSOCIATED CONTENT

Supporting Information

The Supporting Information is available free of charge on the ACS Publications website at DOI: 10.1021/jacs.5b07232.

Hydroxide and excess proton model parameters and details; definitions and details for the local energy decomposition; water coordination numbers of our hydroxide and proton models; comparison with the results of van der Spoel et al. (PDF)

AUTHOR INFORMATION

Corresponding Author

*gavoth@uchicago.edu

Notes

The authors declare no competing financial interest.

ACKNOWLEDGMENTS

This research was funded by the Department of Defense Multidisciplinary University Research Initiative (MURI) through the United States Army Research Office under grant number W911NF-10-1-0520 and the National Science Foundation (NSF grants CHE-1465248 and CHE-1214087). S.T. acknowledges the Croucher Foundation for a postdoctoral research fellowship. C.C. thanks the financial support from the National Natural Science Foundation of China (Grants 21303123 and 21303124) and the China Scholarship Council (No. 201306275019). We thank Dr. Chris Knight of Argonne National Laboratory for his suggestions and comments. Computational resources were purchased with a Defense University Research Instrumentation Program also awarded through the Army Research Office. Additionally this work used resources provided by both the University of Chicago Research Computing Center (RCC) and the U.S. Department of Defense (DOD) High Performance Computing Modernization Program at the Engineer Research and Development Center (ERDC) and the U.S. Air Force Research Laboratory (AFRL).

REFERENCES

(1) Jungwirth, P.; Tobias, D. J. *Chem. Rev.* **2006**, *106*, 1259.
(2) Baer, M. D.; Kuo, I. F. W.; Tobias, D. J.; Mundy, C. J. *J. Phys. Chem. B* **2014**, *118*, 8364.
(3) Petersen, M. K.; Iyengar, S. S.; Day, T. J. F.; Voth, G. A. *J. Phys. Chem. B* **2004**, *108*, 14804.
(4) Onsager, L.; Samaras, N. N. T. *J. Chem. Phys.* **1934**, *2*, 528.
(5) Petersen, P. B.; Saykally, R. J. *J. Phys. Chem. B* **2005**, *109*, 7976.
(6) Tarbuck, T. L.; Ota, S. T.; Richmond, G. L. *J. Am. Chem. Soc.* **2006**, *128*, 14519.
(7) Levering, L. M.; Sierra-Hernández, M. R.; Allen, H. C. *J. Phys. Chem. C* **2007**, *111*, 8814.
(8) Tian, C.; Ji, N.; Waychunas, G. A.; Shen, Y. R. *J. Am. Chem. Soc.* **2008**, *130*, 13033.
(9) Mucha, M.; Frigato, T.; Levering, L. M.; Allen, H. C.; Tobias, D. J.; Dang, L. X.; Jungwirth, P. *J. Phys. Chem. B* **2005**, *109*, 7617.
(10) Ishiyama, T.; Morita, A. *J. Phys. Chem. A* **2007**, *111*, 9277.
(11) Pegram, L. M.; Record, M. T. *J. Phys. Chem. B* **2007**, *111*, 5411.
(12) Iuchi, S.; Chen, H.; Paesani, F.; Voth, G. A. *J. Phys. Chem. B* **2009**, *113*, 4017.
(13) Kumar, R.; Knight, C.; Voth, G. A. *Faraday Discuss.* **2014**, *167*, 263.
(14) Schmitt, U. W.; Voth, G. A. *J. Chem. Phys.* **1999**, *111*, 9361.
(15) Day, T. J. F.; Soudackov, A. V.; Čuma, M.; Schmitt, U. W.; Voth, G. A. *J. Chem. Phys.* **2002**, *117*, 5839.
(16) Wu, Y.; Chen, H.; Wang, F.; Paesani, F.; Voth, G. A. *J. Phys. Chem. B* **2008**, *112*, 467.

DOI: 10.1021/jacs.5b07232
J. Am. Chem. Soc. 2015, 137, 12610−12616

(17) Burnham, C. J.; Petersen, M. K.; Day, T. J. F.; Iyengar, S. S.; Voth, G. A. *J. Chem. Phys.* **2006**, *124*, 024327.
(18) Pegram, L. M.; Record, M. T., Jr. *Proc. Natl. Acad. Sci. U. S. A.* **2006**, *103*, 14278.
(19) Pegram, L. M.; Record, M. T., Jr *Chem. Phys. Lett.* **2008**, *467*, 1.
(20) Vacha, R.; Buch, V.; Milet, A.; Devlin, P.; Jungwirth, P. *Phys. Chem. Chem. Phys.* **2007**, *9*, 4736.
(21) Buch, V.; Milet, A.; Vácha, R.; Jungwirth, P.; Devlin, J. P. *Proc. Natl. Acad. Sci. U. S. A.* **2007**, *104*, 7342.
(22) Vacha, R.; Horinek, D.; Berkowitz, M. L.; Jungwirth, P. *Phys. Chem. Chem. Phys.* **2008**, *10*, 4975.
(23) Lee, H.-S.; Tuckerman, M. E. *J. Phys. Chem. A* **2009**, *113*, 2144.
(24) Yamaguchi, S.; Kundu, A.; Sen, P.; Tahara, T. *J. Chem. Phys.* **2012**, *137*, 151101.
(25) Duignan, T. T.; Parsons, D. F.; Ninham, B. W. *Chem. Phys. Lett.* **2015**, *635*, 1.
(26) Jagoda-Cwiklik, B.; Cwiklik, L.; Jungwirth, P. *J. Phys. Chem. A* **2011**, *115*, 5881.
(27) Berkelbach, T. C.; Lee, H.-S.; Tuckerman, M. E. *Phys. Rev. Lett.* **2009**, *103*, 238302.
(28) Tse, Y.-L. S.; Knight, C.; Voth, G. A. *J. Chem. Phys.* **2015**, *142*, 014104.
(29) Marinova, K. G.; Alargova, R. G.; Denkov, N. D.; Velev, O. D.; Petsev, D. N.; Ivanov, I. B.; Borwankar, R. P. *Langmuir* **1996**, *12*, 2045.
(30) Beattie, J. K.; Djerdjev, A. M. *Angew. Chem., Int. Ed.* **2004**, *43*, 3568.
(31) Mishra, H.; Enami, S.; Nielsen, R. J.; Stewart, L. A.; Hoffmann, M. R.; Goddard, W. A.; Colussi, A. J. *Proc. Natl. Acad. Sci. U. S. A.* **2012**, *109*, 18679.
(32) Mundy, C. J.; Kuo, I. F. W.; Tuckerman, M. E.; Lee, H.-S.; Tobias, D. J. *Chem. Phys. Lett.* **2009**, *481*, 2.
(33) Hub, J. S.; Wolf, M. G.; Caleman, C.; van Maaren, P. J.; Groenhof, G.; van der Spoel, D. *Chemical Science* **2014**, *5*, 1745.
(34) Wick, C. D.; Dang, L. X. *J. Phys. Chem. A* **2009**, *113*, 6356.
(35) Wick, C. D.; Dang, L. X. *J. Chem. Phys.* **2010**, *133*, 024705.
(36) Raymond, E. A.; Richmond, G. L. *J. Phys. Chem. B* **2004**, *108*, 5051.
(37) Petersen, P. B.; Saykally, R. J. *Chem. Phys. Lett.* **2008**, *458*, 255.
(38) Imamura, T.; Ishiyama, T.; Morita, A. *J. Phys. Chem. C* **2014**, *118*, 29017.
(39) Saykally, R. *Chem. Phys. Lett.* **2009**, *481*, 1.
(40) Saykally, R. J. *Nat. Chem.* **2013**, *5*, 82.
(41) Agmon, N. *Chem. Phys. Lett.* **1995**, *244*, 456.
(42) Yoo, S.; Zeng, X. C.; Xantheas, S. S. *J. Chem. Phys.* **2009**, *130*, 221102.
(43) Yoo, S.; Xantheas, S. S. *J. Chem. Phys.* **2011**, *134*, 121105.
(44) Knight, C.; Lindberg, G. E.; Voth, G. A. *J. Chem. Phys.* **2012**, *137*, 22A525.
(45) Grimme, S. *J. Comput. Chem.* **2004**, *25*, 1463.
(46) Botti, A.; Bruni, F.; Imberti, S.; Ricci, M. A.; Soper, A. K. *J. Chem. Phys.* **2004**, *121*, 7840.
(47) Park, K.; Lin, W.; Paesani, F. *J. Phys. Chem. B* **2012**, *116*, 343.
(48) Wu, Y.; Tepper, H. L.; Voth, G. A. *J. Chem. Phys.* **2006**, *124*, 024503.
(49) Plimpton, S. *J. Comput. Phys.* **1995**, *117*, 1.
(50) Hockney, R. W.; Eastwood, J. W. *Computer Simulation Using Particles*; Adam Hilger: New York, 1989.
(51) Frenkel, D.; Smit, B. *Understanding Molecular Simulation: From Algorithms to Applications*; Academic Press: San Diego, CA, 2002.
(52) Grossfield, A., WHAM: The Weighted Histogram Analysis Method v. 2.0.9, http://membrane.urmc.rochester.edu/content/wham.
(53) Otten, D. E.; Shaffer, P. R.; Geissler, P. L.; Saykally, R. J. *Proc. Natl. Acad. Sci. U. S. A.* **2012**, *109*, 701.
(54) One reason why the *z*-dependence is needed is that the ion influence of hydronium or hydroxide on the water−water or ion−water interaction energies as a function of radial distance to the ion does not necessarily have spherical symmetry. This nonspherical nature is more pronounced for molecular ions such as hydroxide and hydronium, which have their orientational preference as they approach the surface, than simple monatomic ions. Although the *z*-dependence in the coordination shell (c) region, which is spherical with a fixed radius, partially accounts for the changes in the average interaction energies as a function of *z*, these changes can be better described by also introducing *z*-dependence in the interfacial and bulk regions; what is not included in the c region can be contained in the other two regions because they form a partition of the space. Such changes of the ion influence as a function of *z* directly affect all ion−water energy terms per molecule $\langle E_{iw} \rangle$ in the three regions and the water−water energy term $\langle E_{ww} \rangle$ in the c region, in which the water molecules are right next to the ion.
(55) Willard, A. P.; Chandler, D. *J. Phys. Chem. B* **2010**, *114*, 1954.
(56) In our calculations, we choose the width of the Gaussian function to be 2.4 Å. The instantaneous surface is defined to the surface at density $c = 0.015$ Å^{-3}.

DOI: 10.1021/jacs.5b07232
J. Am. Chem. Soc. 2015, 137, 12610−12616